한국정밀공학회지 제 36 권 제 9 호 pp. 803-811 September 2019 / 803
J. Korean Soc. Precis. Eng., Vol. 36, No. 9, pp. 803-811 https://doi.org/10.7736/KSPE.2019.36.9.803
ISSN 1225-9071 (Print) / 2287-8769 (Online)

Study on Cutting Force and Chip Shrinkage Coefficient during Thermal – Assisted Machining by Induction Heating of SKD11 Steel

Thi-Bich Mac[1,2], Tien-Long Banh[1], and Duc-Toan Nguyen[1,#]

1 School of Mechanical Engineering, Hanoi University of Science and Technology, 1 Dai Co Viet Road, Hanoi, Vietnam
2 Faculty of Mechanical Engineering, Hungyen University of Technology and Education, Hungyen, Vietnam
Corresponding Author / E-mail: toan.nguyenduc@hust.edu.vn, TEL: +84-988-693-047
ORCID: 0000-0001-9619-4476

KEYWORDS: Cutting force, Chip shrinkage coefficient, Thermal – Assisted machining, Induction heating, SKD11 steel

In this work, we present an experimental study on cutting force and chip shrinkage coefficient during the milling of SKD11 steel at elevated temperatures using a high-frequency induction heating method. To improve the determination of the chip shrinkage coefficient, a 3D scanning method incorporating GOM Inspect 3D data analysis software was used to measure the chip length. To evaluate the effect of the heating process on output data such as chip geometry, cutting force, and chip shrinkage coefficient, cutting experiments were conducted at room and elevated temperatures with the same machining parameters of cutting speed, feed rate, and cutting depth. The Taguchi orthogonal array method was subsequently used for experimental design to obtain optimum values of the machining parameters. The analysis of variance method was also performed to indicate the percentage effect of the machining parameters on the cutting force and chip shrinkage coefficient. Finally, models of the cutting force and chip shrinkage coefficient during thermal-assisted milling of SKD11 were established and compared with experimental data.

Manuscript received: February 13, 2019 / Revised: April 4, 2019 / Accepted: May 27, 2019
This paper was presented at PRESM 2019

NOMENCLATURE

F = The synthetic cutting force
Fx, Fy, Fz = Three the cutting forces components
L. L_f = The uncut and actual chip length
F_f = The cutting area
V, f (or f_r), t = Cutting speed, feed rate, cutting depth
K= Chip shrinkage coefficient
Q = Mass of the chip the
ρ = Destiny of the workpiece material
T = Elevated temperature

1. Introduction

Presently, advanced materials show high hardness, less abrasive wear resistance, and thermal conductivity when subjected to elevated temperatures. Moreover, advanced machining methods such as electro-discharge machining, grinding by abrasive diamond, etc., have been developed. However, these machining methods are limited because of low machining productivity due to low material removal rate, expensive tools, fast tool wear, and high machining time.[1,2] Thermal-assisted machining (TAM) is one of the new technological solutions, which supports the cutting process to increase machining productivity, improve surface quality, and reduce cost. Although this method improves machinability, it does not change the material's mechanical properties after the heating process. In TAM, a material is softened, thereby leading to its hardness reduction.[3]

Baili et al.[4] studied the improvement of machinability of Ti-5553 alloy during thermal-assisted turning by a magnetic induction heat source. Studies showed that the cutting force was reduced by 34.4% when the workpiece temperature reached 750°C. Ginta et al.[5] presented the effect of heating process on the cutting ability of Ti-6Al-V4 alloy during thermal-assisted milling on vertical milling

machines. The authors showed that the cutting force, vibration, tool life, and material removal rate is affected by a direct heating process on the machining workpiece. In TAM, a decrease in the cutting force will lead to a reduction of stress on the cutting tool, thereby increasing the tool life and decreasing the vibration of the cutting process. Chip geometry changes when material strength is reduced as proven by Sun et al. during laser-assisted milling of Ti-6Al-V4 alloy.[6] The authors found that chips were segmented in conventional machining. However, the affection of laser heat source, which lead to the reduction of the cutting force, was a significant cause of the transition from segmented to continuous chips in TAM. Chip shrinkage coefficient is an important parameter to evaluate the plasticity deformation of a material. The chip shrinkage coefficient depends on all the factors that affect chip deformation such as mechanical properties, cutting tool geometry, machining parameters, etc..[7] Chip shrinkage coefficient can be recognized as a prominent parameter for controlling and monitoring the cutting process because it reflects changes in the machining parameters or surface finishes quality.[8,9]

To increase productivity and surface quality during the cutting process, an optimized design is widely used for selecting input parameters.[10-13] There are many parameters involved in the optimization design, such as machining parameters, cutter geometry parameters, workpiece material, machining environment, etc. Generally, an optimum cutting condition is based on the experience of the operator or the handbook data. However, in cases of machining a new workpiece material, new machining methods, or a special structural workpiece, the experience/handbook method will not satisfy.

In this study, we present the effect of machining parameters on cutting force and chip shrinkage coefficient in the thermal-assisted milling process of SKD11 steel. The relationships between the cutting force/chip shrinkage coefficient and machining parameters at elevated temperatures are established based on the nonlinear regression tool of Minitab software 17. To obtain optimum cutting and elevated temperature parameters, the Taguchi orthogonal array methods for the design of experiment and analysis of variance (ANOVA) are combined for calculation. Validated experiments were adopted to show agreement with the predicted equations of the cutting force and chip shrinkage coefficient.

2. Experimental Procedures

2.1 Material

In this research, SKD11 steel is used as the workpiece material. This material is widely applied in mold manufacturing industries. Table 1 shows the chemical composition of SKD11 steel.[10]

Table 1 Chemical compositions of SKD11 tool steel (%)

C	Cr	Mo	Si	Mn	Ni	V
1,4-1,6	11-13	0,7-1,2	≤ 0,6	≤ 0,6	-	0,15-0,3

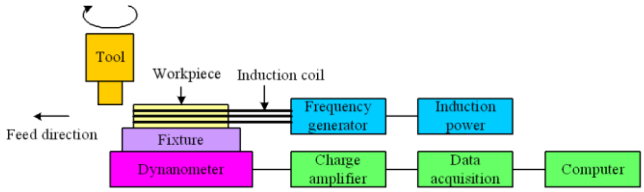

(a)

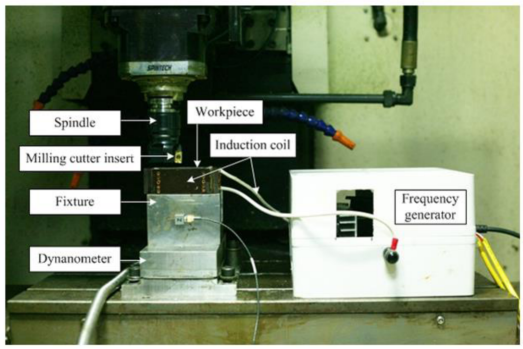

(b)

Fig. 1 Experimental set-up (a) Schematic diagram and (b) experimental photograph

2.2 Experimental Setup

The experimental set-up for thermal-assisted milling of SKD11 steel is shown in Fig. 1. Experiments were conducted on an MC500 milling machine without any lubricant or cooling. A cutting tool (APKT 1604PDR-GM, PRAMET, Czech Republic) with carbide inserts of diameter 40 mm was used. Induction temperature was created using 84 kHz of high-frequency power generated by magnetic induction heating equipment: induction power and frequency generator.

In this study, after each cutting experiment, the carbide inserts were replaced by new ones to avoid the influence of tool wear on the experimental results.

The cutting force was monitored by a piezoelectric force dynamometer (Kistler 9257B), which can measure three orthogonal cutting force components (Fx, Fy, and Fz). The dynamometer is connected to a charge amplifier for amplifying the output voltages, which are proportional to the measuring forces. Subsequently, an acquisition system with DASYlab 10.0 software is used to save the data on a computer.

2.3. Magnetic Induction Heating Process

In the magnetic induction heating process, induction heat is generated by modifying the induction current within the

workpiece. Alternating current is applied to the coil to generate induction current within the workpiece. The intensity of the current is determined by the magnetic flux depending on the permeability (conductivity of the magnetic field) and resistivity of the material (electrical resistance of the electric current).

In general, a transient (time-dependent) heat transfer process in a metal workpiece can be described by the Fourier equation given as Eq. (1).

$$c\rho\frac{\partial T}{\partial t}+\nabla\cdot(-k\nabla T)=Q \tag{1}$$

where T, ρ, c, and k are the temperature (°C), density (g/cm^3), specific heat (J/(kg.K)), and thermal conductivity of the material (W/(m.K)), respectively, and Q is the heat source density induced by the eddy currents per unit time on a unit volume. This heat source is determined by solving electromagnetic problems.

In most cases of TAM by induction heating, boundary conditions are heat losses due to radiation and convection. Hence, the boundary condition is expressed as Eq. (2).

$$-k\frac{\partial T}{\partial n}=\alpha(T_S-T_\alpha)+C_S\left({T_S}^4-{T_\alpha}^4\right)+Q_S \tag{2}$$

where $\partial T/\partial n$ is the temperature gradient in a direction normal to the surface at the point under consideration; α, CS, and QS correspond to the convection surface heat transfer coefficient, radiation heat loss coefficient, and surface loss; and n is the boundary surface symbol.

Eq. (1) can be expressed in Cartesian coordinates as Eq. (3)

$$c\rho\frac{\partial T}{\partial t}=\frac{\partial}{\partial x}\left(k\frac{\partial T}{\partial x}\right)+\frac{\partial}{\partial y}\left(k\frac{\partial T}{\partial y}\right)+\frac{\partial}{\partial z}\left(k\frac{\partial T}{\partial z}\right)+Q \tag{3}$$

Eq. (3) with boundary conditions (Eq. (2)) represents the mathematical model of the heat transfer process in magnetic induction heating and heat transfer applications.

Lei Zhang[14] applied the heat transfer equation to simulate the heat transfer process during magnetic induction heating using COMSOL finite element software. The effect of different parameters on the heat transfer process was also investigated.

In this study, the workpiece temperature is controlled by a hand-held digital contact thermometer (model 3527A from TSURUGA, Japan). The thermometer uses K type thermocouples with a temperature range of −99 to 1299°C. The frequency of results displayed is 2 s^{-1}. In the range of 0 to 400°C, the error of the device is ± (0.2% RDG + 0.5°C).

2.4 Chip Shrinkage Coefficient Determination

The change in the thickness of the uncut chip due to plastic deformation is evaluated by the chip shrinkage coefficient (K), which depends on all the factors that affect the chip deformation: mechanical properties of the workpiece, geometry of the cutting tool, machining parameters, and other cutting conditions. If the volume of the metal block before and after deformation is constant, the chip width when the angle λ is small (λ < 30°) varies insignificantly compared to the cut width. K is determined by Eq. (4).[7]

$$K=\frac{L}{L_f} \tag{4}$$

where L and L_f are the uncut chip and the actual chip length, respectively. Because of the difficulty in the determination of uncut chip length, the method of weight measurement is usually used as follows:

The cutting area is:

$$F_f=\frac{1000Q}{\rho L_f} \tag{5}$$

where Q and ρ are the mass of the chip (g) and destiny of the workpiece material (g/cm^3), respectively.

Because the volume of the chip is constant, we have

$$L_f\cdot F_f=L\cdot f_r\cdot t \tag{6}$$

where f_r and t are the feed rate (mm/rev) and cutting depth (mm), respectively.

By substituting Eqs. (6) in (4), K is determined as follows:

$$K=\frac{F_f}{f_r\cdot t} \tag{7}$$

By substituting Eqs. (5) in (7), K is determined as follows:

$$K=\frac{1000Q}{\rho L_f f_r t} \tag{8}$$

In this study, chip length was measured using a 3D scanning method incorporating GOM Inspect Professional 3D data analysis software for high accuracy. The chips were scanned by ATOS Core 80 3D scanners on an ATOS ScanPort system (Fig. 2). This is an automated system that measures and tests small details with six kinematics combined movement around work points. The three motorized axes are the tilting, rotation, and linear axes. The three manual axes are an eccentric plate (eccentric adjustment with two degrees of freedom), a sensor axis (stepless rotation around sensor axis 0-90°), and an adapter for height variation. ATOS Core 80 uses blue light technology, which provides high accuracy, and the scan results are not affected by ambient light owing to different light

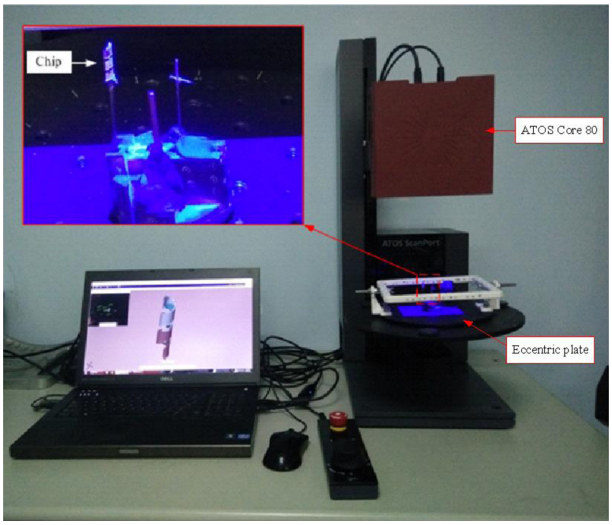

Fig. 2 The ATOS scan port system

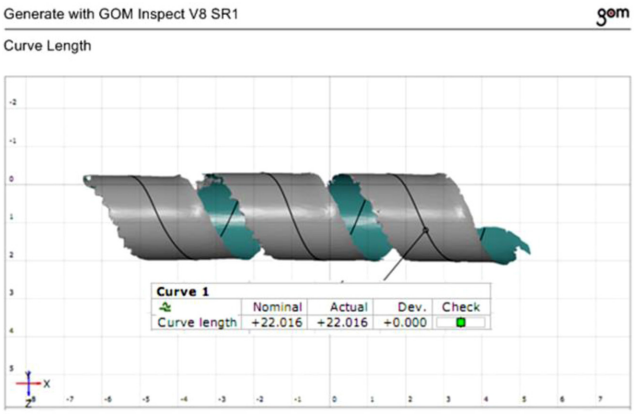

Fig. 3 Result of chip length measurement

frequencies. Subsequently, GOM Inspect 3D data analysis software is used to analyze the data and measure the chip length as shown in Fig. 3.

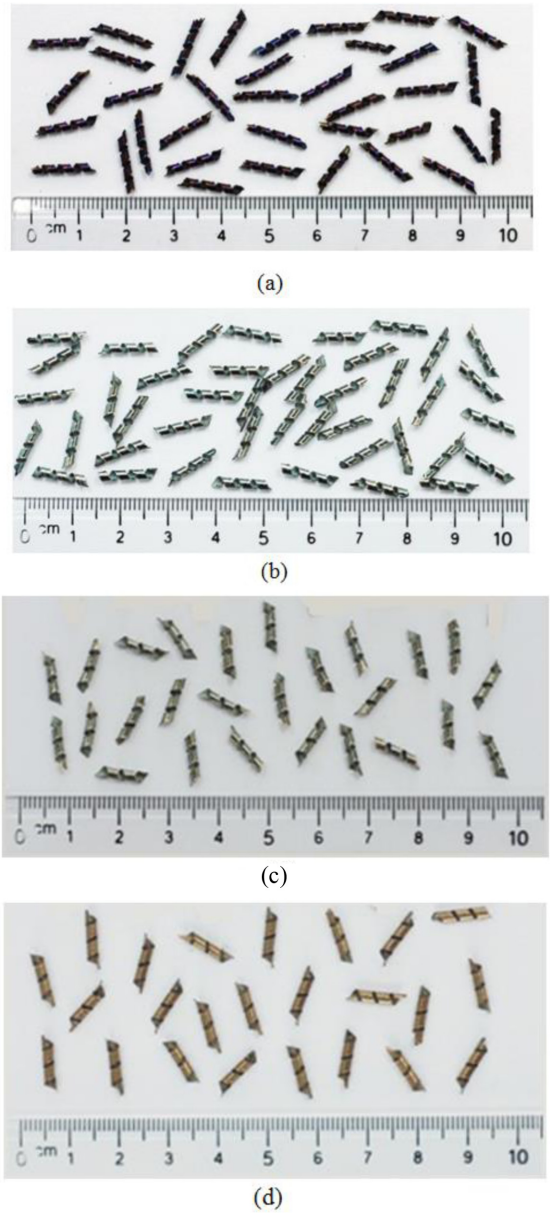

Fig. 4 Chip morphology during conventional machining (a) and TAM at 200°C (b), 300°C (c), and 400°C (d)

3. Results and Discussions

3.1 Chip Morphology

Figs. 4(a)-4(d) show the chip morphology of the milling of SKD11 steel with machining parameters (V = 235 m/min, f = 305 mm/min, and t = 1.5 mm) at room temperature and 200, 300, and 400°C, respectively. Continuous chips are formed by the plasticity characteristics of the workpiece material. However, a chip's color is completely different in traditional machining than that in TAM. In traditional machining, a chip's color is dark purple due to the heat generated and transferred from the heating sources to the chip. However, in TAM, the color of a chip is much brighter because the cutting temperature was pre-elevated, thereby causing more uniform heat transfers to the chip.

3.2 Effect of Heating Process on Cutting Force and Chip Shrinkage Coefficient

Fig. 5 shows the experimental results of the dependence of cutting force on the cutting speed at elevated temperatures. Table 2 presents the cutting force and chip shrinkage coefficient values at various cutting speeds and temperatures. The results show that the cutting force reduces remarkably during TAM at 200°C compared to that during conventional machining. The cutting force reduces when the temperature is increased to 300 and 400°C. ΔF is the

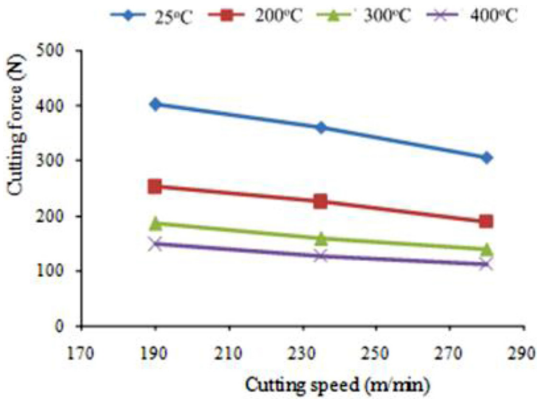

Fig. 5 The cutting force depends on cutting speed (V) and temperature (T)

Table 2 The cutting force and chip shrinkage coefficient are during machining at various cutting speeds and temperatures

V (m/min)	F (N)			
	T= 25°C	T= 200°C	T= 300°C	T= 400°C
190	405.6342	250.9870	184.7650	142.7787
235	360.1700	224.9620	159.6134	125.7869
280	298.8975	189.8791	135.5634	110.9098
V (m/min)	K			
	T= 25°C	T= 200°C	T= 300°C	T= 400°C
190	1.2045	1.4985	1.5234	1.6324
235	1.1325	1.4451	1.5456	1.6587
280	1.0721	1.4236	1.4876	1.5234

percentage of cutting force reduction determined using Eq. (9). The maximum ΔF is 65.1% during TAM at 400°C and a 235 m/min of cutting speed (V). Hence, higher the temperature (T), lower is the cutting force (F). The strength and hardness of a material reduce because of the effect of elevated temperatures during heating. The bonding force between metal atoms becomes weak, thereby making the cutting process easy. The main reason is the softening effect caused by heating the workpiece material during the machining process. In general, the temperature of the primary shear zone increases when (V) increases. Hence, (F) is reduced by decreasing the flow stress in the primary shear zone. Besides, when (V) increases, the contact area between the rake surface of a tool and chip is reduced leading to decreasing frictional force.

$$\Delta Y(\%) = \frac{|Y_T - Y_R|}{Y_R} \cdot 100\% \quad (9)$$

where Y_T and Y_R are the cutting force or chip shrinkage coefficient during TAM and conventional machining, respectively.

Fig. 6 presents the effect of cutting speed (V) and elevated

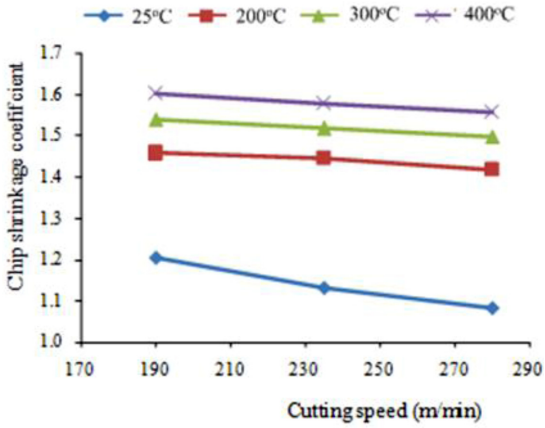

Fig. 6 The chip shrinkage coefficient depends on cutting speed (V) and temperature (T)

temperature (T) on the chip shrinkage coefficient. The effect of (V) on the chip shrinkage coefficient is the same as that on the cutting force; thus, the chip shrinkage coefficient decreases when (V) increases. On the other hand, when temperature increases, the chip shrinkage coefficient also increases. The increase in the chip shrinkage coefficient (ΔK) is determined using Eq. (9). The results show that the maximum ΔK is 31.7% during TAM at 400°C and the cutting speed of 235 m/min. Because the material is softened under the influence of elevated temperature, the bonding between atoms becomes weak; thus, the arrangement of the metal lattice can be destroyed easily. Hence, a workpiece material will be easily deformed if the chip shrinkage coefficient is high.

3.3 Optimization of Cutting Parameters

In this study, cutting parameters such as cutting speed (V), feed rate (f), cutting depth (t), and elevated temperature (T) are selected. Their optimal values (V, f, t, and T) will be chosen for the objective function of cutting force and chip shrinkage coefficient. Besides, the contribution percentage of the parameters will be assessed by the ANOVA method.

Taguchi proposed the signal to noise (S/N) ratio as the representative value to choose level, which is the best noise control. The S/N ratio considers both the mean and variation depending on the behavior of the target. The simplest form of the S/N ratio is the ratio of the mean (signal) to the standard deviation (noise). Because the optimization study for the objective function is the cutting force and chip shrinkage coefficient, the S/N ratio with smaller is better criteria is chosen. The formula for calculating the S/N ratio is given in Eq. (10)[15]:

$$X = -10log\frac{1}{n}\sum_{i=1}^{n} y_i{}^2 \quad (10)$$

Table 3 Parameters with levels

Symbol	Control parameter	Unit	Level		
			1	2	3
A	Cutting speed (V)	m/min	190	235	280
B	Feed rate (f)	mm/min	230	305	380
C	Cutting depth (t)	mm	0.5	1	1.5
D	Temperature (T)	°C	200	300	400

Table 4 The orthogonal array L9.

Trial No.	V (m/min)	f (mm/min)	t (mm)	T (°C)
1	190	230	0.5	200
2	190	305	1	300
3	190	380	1.5	400
4	235	230	1	400
5	235	305	1.5	200
6	235	380	0.5	300
7	280	230	1.5	300
8	280	305	0.5	400
9	280	380	1	200

Table 5 The observed values are calculated

Trial No.	Cutting force		Chip shrinkage coefficient	
	F	X(F)	K	X(K)
1	62.205	-35.8765	1.6539	-4.37032
2	129.917	-42.2733	1.6056	-4.11278
3	155.140	-43.8145	1.4328	-3.12343
4	90.248	-39.1087	1.7531	-4.87623
5	224.962	-47.0422	1.4451	-3.19792
6	74.014	-37.3862	1.2253	-1.7651
7	112.068	-40.9897	1.7013	-4.61541
8	39.256	-31.8781	1.6314	-4.25132
9	134.258	-42.5588	1.2802	-2.14575

where n is the number of repeated experiments and $\sum_{i=1}^{n} y_i^2$ is the sum of the square of all the results for each experiment.

Table 3 presents the parameters with their corresponding levels. The three selected parameters (V, f, and t) combined with the heating temperature contributed to the greatest effect on the cutting process. Table 4 shows the orthogonal array L9 according to the Taguchi method. The experimental results of the cutting force and chip shrinkage coefficient with the S/N ratio of each corresponding experiment are calculated using Eq. (10) and shown in Table 5. ANOVA result for the cutting force (F) is presented in Table 6. As observed, the percentage contribution of the cutting depth (t) is the highest at 67%, while that of the supported temperature (T) and

Table 6 Results of ANOVA for F

Factor	Mean S/N ratio of each level			The total squared	Contribution
	1	2	3		
A	-40.65	-41.18	-38.48*	1812	0.072
B	-38.66*	-40.40	-41.25	3058	0.122
C	-35.05*	-41.31	-43.95	16810	0.670
D	-41.83	-40.22	-38.27*	3423	0.136

*Optimum level

Table 7 Results of ANOVA for chip shrinkage coefficient (K)

Factor	Mean S/N ratio of each level			The total squared	Contribution
	1	2	3		
A	-3.869	-3.288*	-3.671	0.013	0.046
B	-4.621	-3.854	-2.345*	0.234	0.827
C	-3.462	-3.712	-3.646*	0.003	0.011
D	-3.238*	-3.498	-4.084	0.033	0.117

*Optimum level

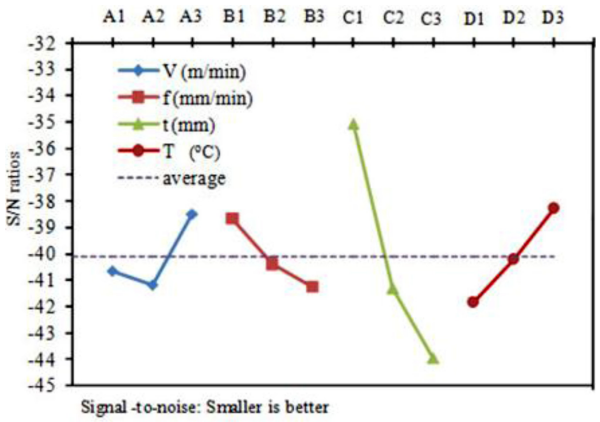

Fig. 7 Mean of S/N ratios of the factors considering F

feed rate (f) are lower at 13.6 and 12.2%, respectively. The cutting speed (V) has a negligible effect on the cutting force with a contribution percentage of 7.2%. Fig. 7 shows the S/N ratio response. The optimal conditions for F are A3B1C1D3 with V = 280 m/min, f = 230 mm/min, t = 0.5 mm, and T = 400°C.

Table 7 presents the ANOVA result for the chip shrinkage coefficient (K). The results show that the percentage contribution of the feed rate (f) was the highest at 82.7%, while that of the supported temperature (T) and cutting speed (V) are lower at 11.7 and 4.6%, respectively. The cutting depth (t) has negligible effect on the chip shrinkage coefficient with a contribution percentage of 1.1%. The S/N ratio response is shown in Fig. 8. The optimal conditions for K are A2B3C1D1 with V = 235 m/min, f = 380 mm/min, t = 0.5 mm, and T = 200°C.

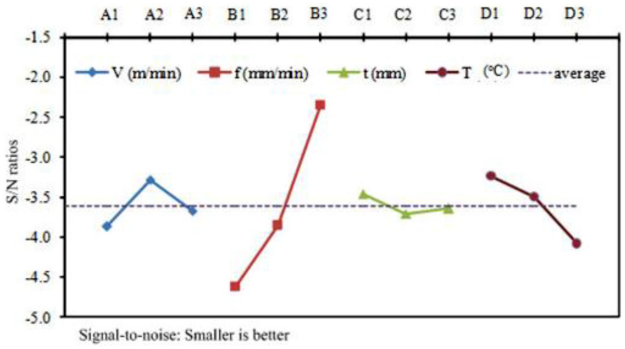

Fig. 8 Mean of S/N ratios of the factors considering K

Table 8 The coefficients and exponents of the cutting force and chip shrinkage coefficient model

Coefficient	a_1	b_1	c_1	d_1	e_1
Value	36235.7	-0.737867	0.453832	0.964106	-0.770712
Coefficient	a_2	b_2	c_2	d_2	e_2
Value	16.9238	-0.071819	-0.489535	0.011429	0.135969

3.4 The Cutting Force and the Chip Shrinkage Coefficient Models

The cutting force and chip shrinkage coefficient models depend on the technological parameters (V, f, and t) and supported temperature for the machining process (T) and are described by Eqs. (11) and (12), respectively.

$$F = a_1 \cdot V^{b_1} \cdot f^{c_1} \cdot t^{d_1} \cdot T^{e_1} \quad (11)$$

$$K = a_2 \cdot V^{b_2} \cdot f^{c_2} \cdot t^{d_2} \cdot T^{e_2} \quad (12)$$

where a_1 and a_2 are coefficients; b_1, c_1, d_1, e_1 and b_2, c_2, d_2, e_2 are the exponents determined from the experiments; and F is the synthetic cutting force analyzed by the three cutting force components (Fx, Fy, and Fz) according to Eq. (13).

$$F = \sqrt{F_x^2 + F_y^2 + F_z^2} \quad (13)$$

In this study, the Gauss–Newton method is used to construct a nonlinear regression function of the cutting force and chip shrinkage coefficient models. This method is applied in the nonlinear regression tool of Minitab 17 software. The results of cutting force and chip shrinkage coefficient presented in Tables 4 and 5, respectively, obtained from the experiments and the orthogonal array L9 are used as input data for the method. The values of the coefficients and exponents are listed in Table 8.

The nonlinear regression functions of the cutting force and chip shrinkage coefficient during the TAM of SKD11 steel are given by Eqs. (14) and (15), respectively.

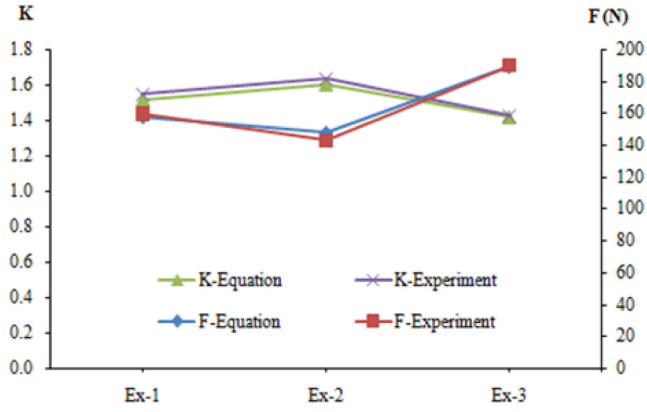

Fig. 9 Comparing the experimental and numerical of the cutting force and the chip shrinkage coefficient value

$$F = 36235.7 \cdot V^{-0.737867} \cdot f^{0.453832} \cdot t^{0.964106} \cdot T^{-0.770712} \quad (14)$$

$$K = 16.9238 \cdot V^{-0.071819} \cdot f^{-0.489535} \cdot t^{0.011429} \cdot T^{0.135969} \quad (15)$$

To evaluate the accuracy of the cutting force and chip shrinkage coefficient models, extra experimental data was used as shown in Fig. 9, where: experiment 1, 2, 3 (Ex-1, Ex-2, Ex-3) were performed at the fixed feed rate of 305 mm/min and the fixed cutting depth of 1.5 mm while the cutting speed and elevated temperature were corresponding at (235 m/min, 300°C), (190 m/min, 400°C) and (280 m/min, 200°C), respectively. The results show that the graph, which is built using the experimental data, is similar to the one built using the numerical data. Hence, the cutting force and chip shrinkage coefficient models represented by Eqs. (14) and (15), respectively, have high accuracy.

By using Eqs. (14) and (15) and the Maple software tool, Figs. 10 and 11 were also built to present the relationship between the cutting force/chip shrinkage coefficient and the machining parameters at elevated temperatures. Fig. 10 shows that when the temperature for the machining process is high, the cutting force is low. Figs. 10(a)-10(c) show the cutting force at fixed (V), (f) and (t), respectively, and the slope of the cutting force graph is maximum when changing (t). Hence, cutting depth has the greatest effect on the cutting force. Fig. 10(c) shows the slope of the cutting force graph when the change in (V) is higher than that in (f). This means that the contribution percentage of (V) is higher than that of (f) on the cutting force (F).

Fig. 11 presents the relationship between the chip shrinkage coefficient (K) and machining parameters and shows that high temperatures lead to large chip shrinkage coefficient values. Figs. 11(a) and 11(c) are graphs of the chip shrinkage coefficient at fixed (V) and (t), respectively, indicating the increasing chip shrinkage coefficient with changing (f). Thus, (f) makes a major contribution

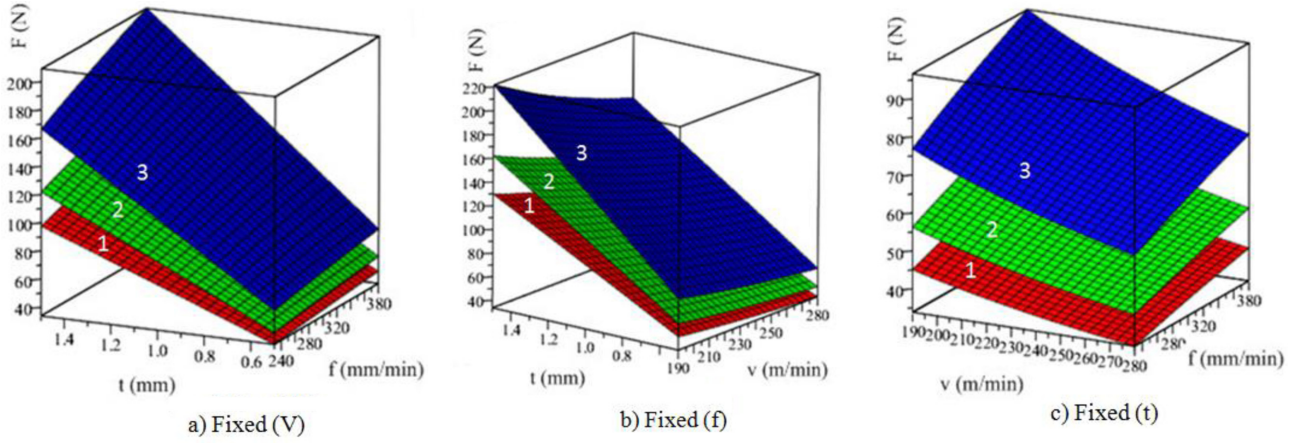

Fig. 10 The relationship between the cutting force (F) and technological parameters (The graphs are labeled 1, 2, 3 in order of roughness graph at 200°C, 300°C, and 400°C)

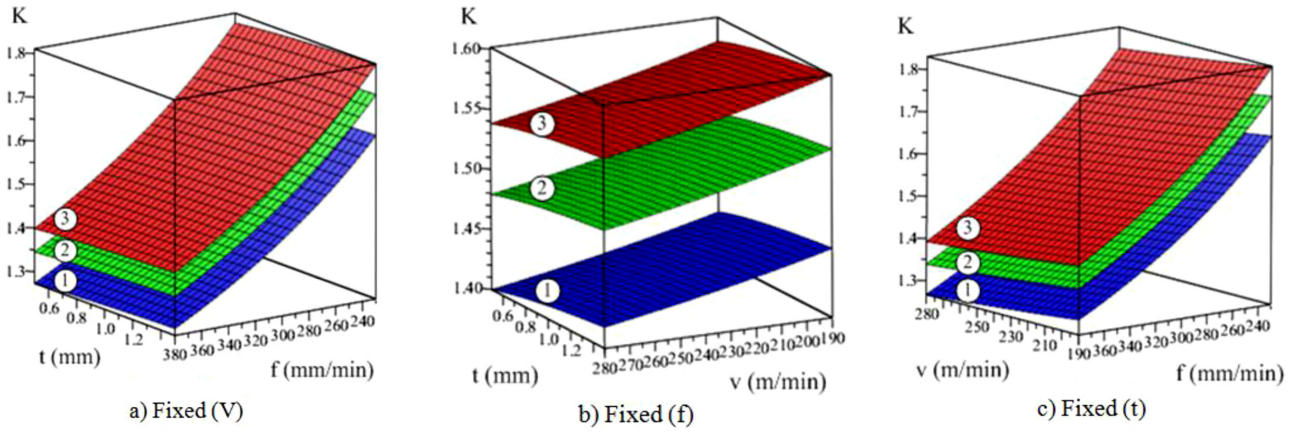

Fig. 11 The relationship between chip shrinkage coefficient (K) and machining parameters (The graphs are labeled 1, 2, 3 in order of roughness graph at 200°C, 300°C, and 400°C)

to (K). Fig. 11(c) is the chip shrinkage coefficient graph at a fixed (f) showing that (f) and (t) have negligible influence on K.

4. Conclusions

A study on the cutting force and chip shrinkage coefficient during the TAM by induction heating of tool steel SKD11 is presented in this study. By heating the workpiece before machining, the cutting force reduced and the chip shrinkage coefficient increased because of the softened material. The level of effect of each parameter and the optimal conditions for the cutting force and chip shrinkage coefficient were determined. The equations of the cutting force and chip shrinkage coefficient, which depend on the cutting parameters and elevated temperature, were established and they showed good agreement with the experimental data.

REFERENCES

1. Benga, G. C. and Abrao, A. M., "Turning of Hardened 100CR6 Bearing Steel with Ceramic and PCBN Cutting Tools," Journal of Materials Processing Technology, Vols. 143-144, pp. 237-241, 2003.

2. Chinchanikar, S. and Choudhury, S. K., "Effect of Work Material Hardness and Cutting Parameters on Performance of Coated Carbide Tool when Turning Hardened Steel: An Optimization Approach," Measurement, Vol. 46, No. 4, pp. 1572-1584, 2013.

3. Brecher, C., Emonts, M., Rosen, C.-J., and Hermani, J.-P., "Laser-Assisted Milling of Advanced Materials," Physics Procedia, Vol. 12, pp. 599-606, 2011.

4. Baili, M., Wagner, V., Dessein, G., Sallaberry, J., and Lallement, D., "An Experimental Investigation of Hot Machining with Induction to Improve Ti-5553 Machinability," Applied Mechanics and Materials, Vol. 62, pp. 67-76, 2011.

5. Ginta, T. L. and Amin, A. N., “Thermally-Assisted End Milling of Titanium Alloy Ti-6Al-4V Using Induction Heating,” International Journal of Machining and Machinability of Materials, Vol. 14, No. 2, pp. 194-212, 2013.
6. Sun, S., Brandt, M., and Dargusch, M., “The Effect of a Laser Beam on Chip Formation During Machining of Ti-6Al-4V Alloy,” Metallurgical and Materials Transactions A, Vol. 41, No. 6, pp. 1573-1581, 2010.
7. Pham, T.-H., Mac, T.-B., Tong, V.-C., Banh, T.-L., and Nguyen, D.-T., “A Study on the Cutting Force and Chip Shrinkage Coefficient in High-Speed Milling of A6061 Aluminum Alloy,” The International Journal of Advanced Manufacturing Technology, Vol. 98, Nos. 1-4, pp. 177-188, 2018.
8. Pham, T.-H., Mac, T.-B., Tong, V.-C., Banh, T.-L., and Nguyen, D.-T., “Simulation and Experimental Studies to Verify the Effect of Cutting Parameters on Chip Shrinkage Coefficient and Cutting Forces in Machining of A6061 Aluminum Alloy,” Advances in Mechanical Engineering, Vol. 8, No. 10, 2016. (DOI: 10.1177/1687814016673297)
9. Mac, T.-B., Dinh, V.-C., Banh, T.-L., and Nguyen, D.-T., “Cutting Force Model for Thermal-Assisted Machining of Tool Steel based on the Taguchi Method,” Metals, Vol. 8, No. 12, Paper No. 992, 2018.
10. Hasçalık, A. and Çaydaş, U., “Optimization of Turning Parameters for Surface Roughness and Tool Life based on the Taguchi Method,” The International Journal of Advanced Manufacturing Technology, Vol. 38, Nos. 9-10, pp. 896-903, 2008.
11. Mukherjee, I. and Ray, P. K., “A Review of Optimization Techniques in Metal Cutting Processes,” Computers & Industrial Engineering, Vol. 50, Nos. 1-2, pp. 15-34, 2006.
12. Wang, C., Xie, Y., Zheng, L., Qin, Z., Tang, D., et al., “Research on the Chip Formation Mechanism during the High-Speed Milling of Hardened Steel,” International Journal of Machine Tools and Manufacture, Vol. 79, pp. 31-48, 2014.
13. Zhang, L., “Numerical Modeling of Induction Assisted Subsurface Heating Technology,” Ph.D. Thesis, Worcester Polytechnic Institute, 2012.
14. Roy, R. K., “A Primer on the Taguchi Method,” Van Nostrand Reinhold, New York, 1990.

Thi-Bich Mac
Ph.D candidate in the School of Mechanical Engineering, Hanoi University of Science and Technology, Vietnam. Her research interests are CAD/CAM/CAE, forming and Machining process.
E-mail: bich.utehy@gmail.com

Tien-Long Banh
Professor in the School of Mechanical Engineering, Hanoi University of Science and Technology, Vietnam. His research interests are Metal cutting, industrial instrument, CAD/CAM/CAE
E-mail: long.banhtien@hust.edu.vn

Duc-Toan Nguyen
Associate Professor in the School of Mechanical Engineering, Hanoi University of Science and Technology, Vietnam. His research interests are Plasticity, Machining Process, CAD/CAM/CAE.
E-mail: toan.nguyenduc@hust.edu.vn